Mixing Temperatures of Bilayers Not Simply Related to Thickness Differences between L_o and L_d Phases

Joan V. Bleecker,[1] Phillip A. Cox,[1] and Sarah L. Keller[1,*]

[1]Department of Chemistry, University of Washington, Seattle, Washington

ABSTRACT Micron-scale coexisting L_o and L_d liquid phases can appear in lipid bilayers composed of a ternary mixture of a low-melting temperature lipid, a high-melting temperature lipid, and cholesterol. A priori, temperatures at which membranes demix, T_{mix}, are not simply related to differences in thicknesses, Δh, between L_o and L_d phases. Here, we use fluorescence microscopy to measure T_{mix} and we use atomic force microscopy at 22°C to measure Δh for a series of bilayers composed of different ratios of the three components. Our data illustrate cases in which a change in T_{mix} or Δh does not result in a change in the other parameter. The data provide a context in which to evaluate recent reports of a correlation between T_{mix} and Δh.

Model lipid membranes composed of a high-melting temperature (T_{melt}) lipid, a low-T_{melt} lipid, and a sterol can phase-separate into liquid-ordered (L_o) and liquid-disordered (L_d) phases (1). Typically, the L_o phase is thicker than the L_d phase (2–4), and is sometimes referred to as the "raft phase" by researchers who associate membrane phases with the lipid raft hypothesis (5).

Two important parameters characterizing this phase separation are T_{mix}, the mixing temperature below which L_o and L_d phases appear in the membrane, and Δh, the thickness difference between L_o and L_d phases at a given temperature. Previous studies have shown that a mismatch between L_o and L_d thicknesses affects protein sorting (6), and that bilayer thickness affects protein function (7,8).

Fig. 1 frames possible relationships between Δh and T_{mix}: the variables can vary independently (line *A* or *B*) or be correlated (curve *C*). Previous work by García-Sáez et al. (2) reported that T_{mix} increases with increasing Δh (as in Fig. 1 *C*) for bilayers at a fixed 40:40:20 mol ratio of low-T_{melt} lipid/high-T_{melt} lipid/cholesterol. In their work, the high-T_{melt} lipid was stearoyl-sphingomyelin. Their low-T_{melt} lipids were a series of phosphocholines (PCs) with carbon chains that systematically lengthened from 14:1 (largest T_{mix} and Δh) to 22:1 (smallest T_{mix} and Δh). They reported T_{mix} proportional both to Δh^2 and to line tension.

The results of García-Sáez et al. (2) have been used to support statements that hydrophobic length mismatch between

lipid types promotes their segregation in phase-separated membranes (6) and drives domain formation by increasing line tension (8). However, the quantitative result of García-Sáez et al. (2) holds only for the particular ratio and types of lipids for which it was reported. For a broader class of membrane systems, T_{mix} is not related to Δh (or to line tension) in a simple way. T_{mix} is determined by the shape of the phase boundary and depends on the ratio and type of lipids. Consider an analogy of an ant crawling over a bowl placed upside-down on the floor. Specifying the type of bowl (the types of lipids in the membrane) limits the ant's highest possible elevation (the highest T_{mix}), but does not specify the ant's current elevation (the membrane's T_{mix}) unless the shape of the bowl and the ant's latitude and longitude across the floor (the ratio of lipids in the membrane) are known.

Moreover, the highest T_{mix} can be difficult to predict for a membrane composed of an arbitrary ternary set of lipids (as opposed to the series of García-Sáez et al. (2)). We have found no monotonic relationship between the highest T_{mix} of a ternary membrane and the estimated thickness difference between the L_o and L_d phases at room temperature (4).

Now imagine two ants crawling over two nested bowls. The bowls may be nonaxisymmetric and their centers may be offset. Even if the bowl depths are simply related (e.g., the highest possible elevation of ant 1 is half that of ant 2), and the ants share the same latitude and longitude with respect to the floor, the difference between the ants' elevations is nontrivial to find. This scenario corresponds to the nested phase diagrams in Fig. S1 in the Supporting Material. To give concrete examples, here we use data to illustrate cases in which a change in Δh or T_{mix} does not result in a change in the other parameter, as schematically depicted in Fig. 1, lines *A* and *B*.
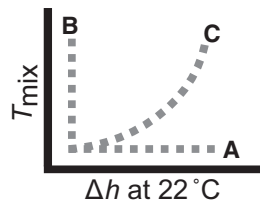
CrossMark

FIGURE 1 Possible trends between thickness mismatch (Δh) and miscibility temperatures (T_{mix}) for membranes that demix into L_o and L_d phases. Data as in curve C appear in García-Sáez et al. (2) and may correspond to Fig. S1, a and b. Here we present data as in lines A and B.

To gather data as in lines *A* and *B* in Fig. 1, we used tactics applicable to any membrane that demixes into L_o and L_d phases. All possible ratios of the three lipid types in a membrane can be plotted in a plane. By definition, a tie-line passes through the overall lipid ratio of any particular membrane. The ends of that tie-line fall at the lipid ratio of that particular membrane's L_o phase, and of its L_d phase. The length and orientation of the tie-line within the plane varies with temperature (9). Two membranes at the same temperature that have different overall ratios of the same lipid types demix into exactly the same L_o and L_d phases if their overall lipid ratios fall on the same tie-line. Along the line, relative areas of the L_o and L_d phases vary.

To observe the trend in line *A* of Fig. 1, our goal was to measure Δh for a series of membranes with lipid ratios that follow an isotherm in T_{mix}. We chose each lipid ratio to fall on a different tie-line. Based on previous work, we hypothesized that membrane compositions that lie on longer tie-lines would produce larger values of Δh (9–11).

To observe the trend in line *B*, our goal was to measure T_{mix} for a series of membranes with lipid ratios that follow a previously determined tie-line at 22°C (9). Because

the composition of the L_o and L_d phases are constant along this line, all of these membranes should share the same Δh.

We determined T_{mix} as the temperature at which 50% of giant unilamellar vesicles (GUVs) demix, as in Fig. 2 *A*. GUVs were composed of mixtures of DPPC (dipalmitoyl-PC), DiPhyPC (diphytanoyl-PC), and cholesterol. They were labeled with 0.8 mol % Texas Red, which partitions preferentially to the L_d phase. GUVs were electroformed and imaged as previously noted in Veatch and Keller (11). We determined Δh from atomic force microscopy (AFM) measurements of supported bilayers. Small unilamellar vesicles were deposited on mica at 60°C in a solution of 5 mM $CaCl_2$ (10). The resulting bilayer was rinsed with 18 MΩ-cm water by pipette and scanned in an atomic force microscope at 22°C. AFM images were flattened in Gwyddion (12). Height histograms were exported to MATLAB (The MathWorks, Natick, MA) and fit with Gaussian peaks as in Fig. 2 (4). Further details of Materials and Methods are in the Supporting Material.

Our central result, namely that T_{mix} and Δh can vary independently, is shown in Fig. 3. Points *a*1–*a*4 in Fig. 3 *A* lie on an isotherm in T_{mix}. Points *b*1–*b*4 in Fig. 3 *B* lie on a tie-line. Because our result follows from general attributes of phase diagrams, it applies to any ternary membrane that demixes into L_o and L_d phases.

Our result reveals difficulties inherent in quantifying relationships between T_{mix} and Δh for membranes made from different lipid species unless full phase diagrams and tie-lines are known. Generalizing from data collected at just one ratio of lipids is meaningful only when phase boundaries for the two systems are related by a simple geometric scaling and are centered at the same ratio of lipids. In addition, either the phase boundary must be hemispherical or the direction of the tie-lines must not change
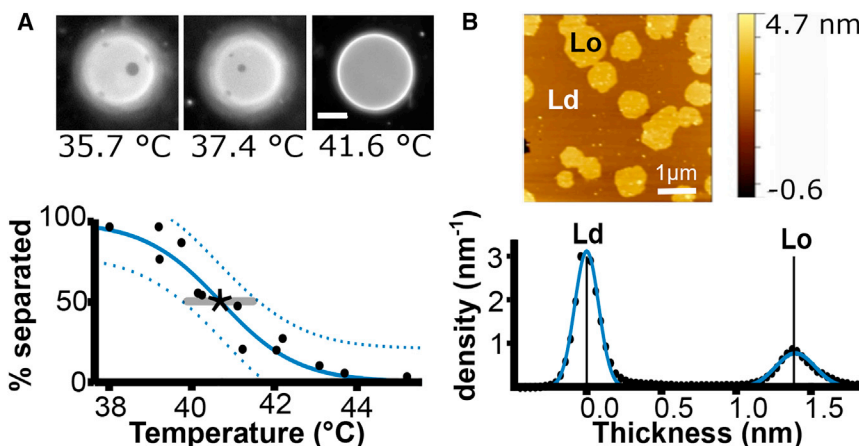

FIGURE 2 Measured values of T_{mix} and Δh for 48:32:20 DiPhyPC/DPPC/chol bilayers. (A) Fluorescence micrographs for a single GUV (*top*) and a graph of percent demixed GUVs versus temperature for a population of GUVs (*bottom*). The solid blue line is a sigmoidal fit of the black points. Dashed lines bound the 95% confidence interval. The star lies at T_{mix}, and the bar spans the uncertainty; here $T_{mix} = 40.7 \pm 0.3$°C. (B) AFM scan of a supported lipid bilayer at 22°C (*top*) and height histogram of the same scan (*bottom*). The blue line follows two Gaussian peak fits of the black data points. For a single scan, Δh is reported as the distance between the mean thicknesses of the two peaks, and uncertainty is reported as the standard deviation of the bootstrap fit, here $\Delta h = 1.39 \pm 0.02$ nm. Values of T_{mix} and Δh are listed in Table S2 in the Supporting Material. To see this figure in color, go online.
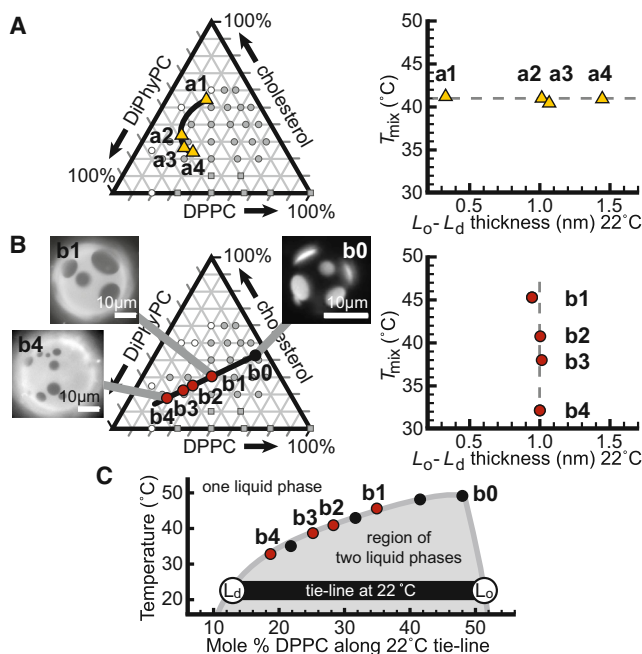
FIGURE 3 Measured values of T_{mix} versus Δh at 22°C for bilayers of DiPhyPC/DPPC/Chol that fall (*A*) on a T_{mix} isotherm and (*B*) on a tie-line. Ternary phase diagrams at 22°C are from Veatch et al. ([9]), where shaded circles denote two liquid phases, open circles denote one liquid phase, and squares denote that a gel phase is present. Micrographs show that area fractions of the L_d phase increases from point *b*0 to *b*4. Dashed lines are not fits. Tables S2–S9 list values and uncertainties. (*C*) Phase boundary along the tie-line in (*B*). Solid points were determined in this study. The underlying shaded curve is not a fit. To see this figure in color, go online.
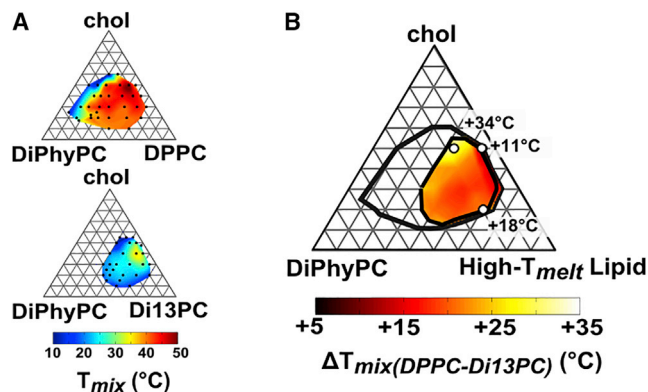

FIGURE 4 (*A*) Phase diagrams for which the high-T_{melt} lipid is either DPPC (with 16 carbons in its acyl chain, *top*) or Di13:0-PC (*bottom*). Black dots are experimental values of T_{mix} including values from Veatch et al. ([9]). The top diagram has higher values of T_{mix} at any lipid ratio and a larger phase boundary at any temperature. (*B*) Difference in T_{mix} (denoted ΔT_{mix}) for GUVs of the two ternary lipid mixtures in (*A*). To see this figure in color, go online.

with temperature (see Fig. S1). We know of no two membrane phase diagrams discovered to date that meet these criteria.

Fig. 4 illustrates this point for two ternary membrane systems for which the high-T_{melt} lipid species differ in the lengths of their acyl chains. Fig. 4 *A* plots T_{mix} values for membranes of DiPhyPC/DPPC/chol and DiPhyPC/Di13:0-PC/chol, where Di13:0-PC has three fewer carbons in each of its two chains than DPPC. The membrane containing DPPC demixes over a broader range of lipid ratios at all temperatures, and its T_{mix} is higher at any lipid ratio at which both membranes demix. A broader range of ratios means longer tie-lines, which can translate into larger Δh ([10]). If we arbitrarily choose any ratio of the three membrane components, we would expect some positive correlation between values of T_{mix} and Δh. However, because the phase boundaries and the tie-lines differ in the two systems, a different choice of this ratio will result in a different quantitative relationship between Δh and T_{mix}. Inherent in this discussion is the perspective that demixing of membranes into phases of different compositions gives rise to Δh and line tension (with values that vary across the phase diagram), and that the value of Δh or line tension at a single

lipid ratio and temperature does not determine the shape of the full phase boundary.

Given that Fig. 3 shows how a single ternary membrane can produce a horizontal or vertical line in a graph of T_{mix} versus Δh, various functional forms relating T_{mix} and Δh for two ternary membranes are then possible, subject to the choice of lipid ratio. Extending this idea, it is possible to imagine future discoveries of membrane systems that produce a negative slope on a graph of T_{mix} versus Δh, as in Fig. S1.

Separately, we can test the correlation between domain size and Δh reported by Heberle et al. ([13]). They used neutron scattering to find that small, 60-nm vesicles with low Δh values had more unmerged domains. They report <2 domains/vesicle for $\Delta h = 0.97$ nm and 23 domains/vesicle for $\Delta h = 0.64$ nm. These Δh values are in line with AFM values from similar lipid systems ([2]). In our GUVs, domains of the same liquid phase merge until only one domain of each phase remains, even when Δh is as small as 0.32 nm. Our results imply that a small Δh value alone does not determine the number of stable, liquid domains.

In conclusion, our results demonstrate challenges of quantitatively establishing how Δh relates to T_{mix}. There is no reason to question the validity of the correlation between Δh and T_{mix} reported by García-Sáez et al. ([2]) for the systems they studied. Nevertheless, Fig. 4 illustrates why other groups are likely to find different values if they employ different ratios of lipids. We also illustrate a method that follows directly from known thermodynamic principles to identify lipid ratios for which T_{mix} and Δh vary independently. We present this method to support future studies of how lipid structure affects T_{mix} and Δh.

SUPPORTING MATERIAL

Supporting Materials and Methods, one figure, and nine tables are available at http://www.biophysj.org/biophysj/supplemental/S0006-3495(16)30276-4.

ACKNOWLEDGMENTS

REFERENCES

1. Veatch, S. L., and S. L. Keller. 2005. Seeing spots: complex phase behavior in simple membranes. *Biochim. Biophys. Acta.* 1746: 172–185.

2. García-Sáez, A. J., S. Chiantia, and P. Schwille. 2007. Effect of line tension on the lateral organization of lipid membranes. *J. Biol. Chem.* 282:33537–33544.

3. Lingwood, D., J. Ries, …, K. Simons. 2008. Plasma membranes are poised for activation of raft phase coalescence at physiological temperature. *Proc. Natl. Acad. Sci. USA.* 105:10005–10010.

4. Bleecker, J. V., P. A. Cox, …, S. L. Keller. 2016. Thickness mismatch of coexisting liquid phases in noncanonical lipid bilayers. *J. Phys. Chem. B.* 120:2761–2770.

5. Lingwood, D., H. J. Kaiser, …, K. Simons. 2009. Lipid rafts as functional heterogeneity in cell membranes. *Biochem. Soc. Trans.* 37: 955–960.

6. Lingwood, D., and K. Simons. 2010. Lipid rafts as a membrane-organizing principle. *Science.* 327:46–50.

7. Cornea, R. L., and D. D. Thomas. 1994. Effects of membrane thickness on the molecular dynamics and enzymatic activity of reconstituted Ca-ATPase. *Biochemistry.* 33:2912–2920.

8. Pike, L. J. 2009. The challenge of lipid rafts. *J. Lipid Res.* 50 (*Suppl*):S323–S328.

9. Veatch, S. L., K. Gawrisch, and S. L. Keller. 2006. Closed-loop miscibility gap and quantitative tie-lines in ternary membranes containing diphytanoyl PC. *Biophys. J.* 90:4428–4436.

10. Connell, S. D., G. Heath, …, A. Kisil. 2013. Critical point fluctuations in supported lipid membranes. *Faraday Discuss.* 161:91–111.

11. Veatch, S. L., and S. L. Keller. 2003. Separation of liquid phases in giant vesicles of ternary mixtures of phospholipids and cholesterol. *Biophys. J.* 85:3074–3083.

12. Nečas, D., and P. Klapetek. 2012. Gwyddion: an open-source software for SPM data analysis. *Open Physics.* 10:181–188.

13. Heberle, F. A., R. S. Petruzielo, …, J. Katsaras. 2013. Bilayer thickness mismatch controls domain size in model membranes. *J. Am. Chem. Soc.* 135:6853–6859.

Supplemental Information

Mixing Temperatures of Bilayers Not Simply Related to Thickness Differences between L_o and L_d Phases

Joan V. Bleecker, Phillip A. Cox, and Sarah L. Keller

Supporting Information: Mixing temperatures of bilayers not simply related to thickness differences between *Lo* and *Ld* phases

Joan V. Bleecker, Phillip A. Cox, and Sarah L. Keller

Department of Chemistry, University of Washington, Seattle, Washington 98195, U.S.A.

Contents

Details of Materials and Methods

   Phospholipids (Avanti Polar Lipids, Alabaster, AL), dye (Texas Red dihexadecanoyl-phosphoethanolamine, DHPE; Life Technologies, Grand Island, NY) and cholesterol (chol; Sigma, St. Louis, MO) were used without further purification. We used only saturated lipids to minimize photooxidation (1). Uncertainty in each single measurement of T_{mix} is reported as a 95% confidence interval of a sigmoidal fit at T_{mix}, as in Fig. 2A of the main text. Measurement uncertainty from sample to sample is on the order of 1 ˚C, given displacements of data points in Fig. 3C from a smooth curve connecting all points.

   Supported lipid bilayers were maintained at 22°C in an AFM chamber. The bilayer was scanned under water on an Asylum Research Cypher ES Environmental AFM system SLD-DD (Asylum Research, Santa Barbara, CA) in tapping mode using blueDrive™ to photothermally drive an Arrow UHFAuD tip (6 N/m, NanoWorld, Neuchâtel, Switzerland) at a resonance frequency of ~400 kHz (rated at 1 MHz in air). The sample chamber was maintained at 22 °C throughout scanning using the built-in temperature controlled stage in the Cypher ES. Measurement uncertainties in Δh are standard deviations from at least three AFM scans for each ratio of lipids, and appear in Table S1.

   T_{mix} was measured in free-floating giant unilamellar vesicles, and Δh was measured in supported lipid bilayers. The presence of a solid substrate has been shown to have only a minor influence on T_{mix} in ternary membranes: the T_{mix} for GUVs of 29.2/32.4/28.4 DiPhyPC/DPPC/chol differs by less than 5˚C from the T_{mix} for GUVs of the same lipid composition deposited on a glass support to produce supported bilayers (2). Evidence that the presence of the solid substrate has only a minor influence on the composition of the L_o and L_d phases is that the area fraction of each phase has been observed to be the same on the surface of a free-floating GUV and in a supported bilayer resulting from deposition and rupture of the same vesicle on a solid support (3) (4).

Discussion of Figure S1

Fig. S1 illustrates points in the main text about lengths of tie-lines in ternary lipid membranes. Membranes composed of at least three lipid types, namely a lipid with a low melting temperature, a lipid with a high melting temperature, and cholesterol or a similar sterol, can demix into coexisting L_o and L_d phases with micron-scale domains.

Each of the panels in Fig. S1 shows miscibility phase boundaries for two different membrane systems, called "red" and "blue". At least one of the three lipid types in the red membrane differs from those in the blue membrane. The ratio of lipid types varies across the x-y plane, and temperature varies along the z-axis. Any point within the volume of the curved surface of the phase boundary corresponds to a membrane that phase separates. Outside of this surface (e.g. at high temperature), all lipids in the membrane mix uniformly.

The four panels schematically represent four possible outcomes of experiments conducted by setting the red and blue membranes at a common ratio of the lipid types and at a common temperature denoted by the black dot). The red (blue) membrane demixes into L_o and L_d phases with lipid ratios that fall at the large red (blue) dots on the x-y plane. The endpoints of the tie-line of the red (blue) membrane fall at these red (blue) dots and the tie-line passes through the black dot. At the tie-line endpoints, the value of T_{mix} is the same as the experimental temperature, whereas in the middle of the tie-line, T_{mix} is higher than the experimental temperature. The shape of each phase boundary is a function of the interaction energies between different types of lipids and the system's entropy. These concepts are reviewed in (5), which gives references to textbooks that discuss phase behavior (6) (7) (8).

The angle between the two tie-lines in the x-y plane is α. The directions of the tie-lines (and hence the angle α between them) are not set by any theoretical constraint; tie-line directions are not known until they are measured, and they change with lipid type and with the experimental temperature (9). This means that the angle α also varies with lipid type and with the experimental temperature.

In only Panel a, the two miscibility phase boundaries are hemispheres offset by a constant height, *d*, which is the difference between the mixing temperatures of the red and blue membranes. The difference between the lengths of the two tie-lines is independent of the angle α if the black dot always lies at the center of the axi-symmetric shapes of the phase boundaries. In the special case of only Panel a, the quantitative relationship between the mixing temperature and tie-line length is generalizable and does not depend on details of the system. To date, no set of two or more membrane miscibility phase boundaries has been documented that fits the constrained characteristics of Panel a.

If the phase boundaries are not axi-symmetric, then a variety of relationships between the demixing temperatures and the lengths of tie-lines are possible as in Panels b-d. The results reported by García-Sáez et al. (10) correspond to Panel b. Panel b is a simplification of known miscibility phase diagrams as in Fig. 4a of the main text and is drawn so that: 1) The two phase boundaries are ellipsoidal; and both ellipses have similar aspect ratios. 2) The black dot

does not lie at the center of both ellipses. 3) The angle α between the tie-lines is nonzero, but small. As a result of these characteristics, tie-line lengths positively correlate with T_{mix} in Panel b, but the quantitative relationship between these two variables changes with the particular choice of lipid ratio (with the placement of the black dot within the x-y plane).

Sets of phase boundaries in which an increase in tie-line length correlates with a *decrease* in T_{mix} are possible to imagine, as in Panels c and d. No experimental systems corresponding to these panels have yet been discovered. In Panel c, the minor axes of the ellipsoidal phase boundaries are much smaller than the major axes, and the tie-lines of the red and blue membranes are nearly perpendicular. In Panel d, the phase boundaries have dissimilar shapes: one is tall and narrow whereas the other is short and broad.

Translating the schematic images in Fig. S1 into plots of T_{mix} vs. Δh for experimental systems is nontrivial because the mapping of tie-line length onto Δh is known for only one system to date (9) (11), and likely depends both on the direction of the tie-line within the *x-y* plane and on the choice of lipid types. To the extent that a difference in lipid composition between the L_{o} and L_{d} phases at a given temperature determines the miscibility phase boundary and (separately) Δh, there exists a relationship between T_{mix} and Δh.
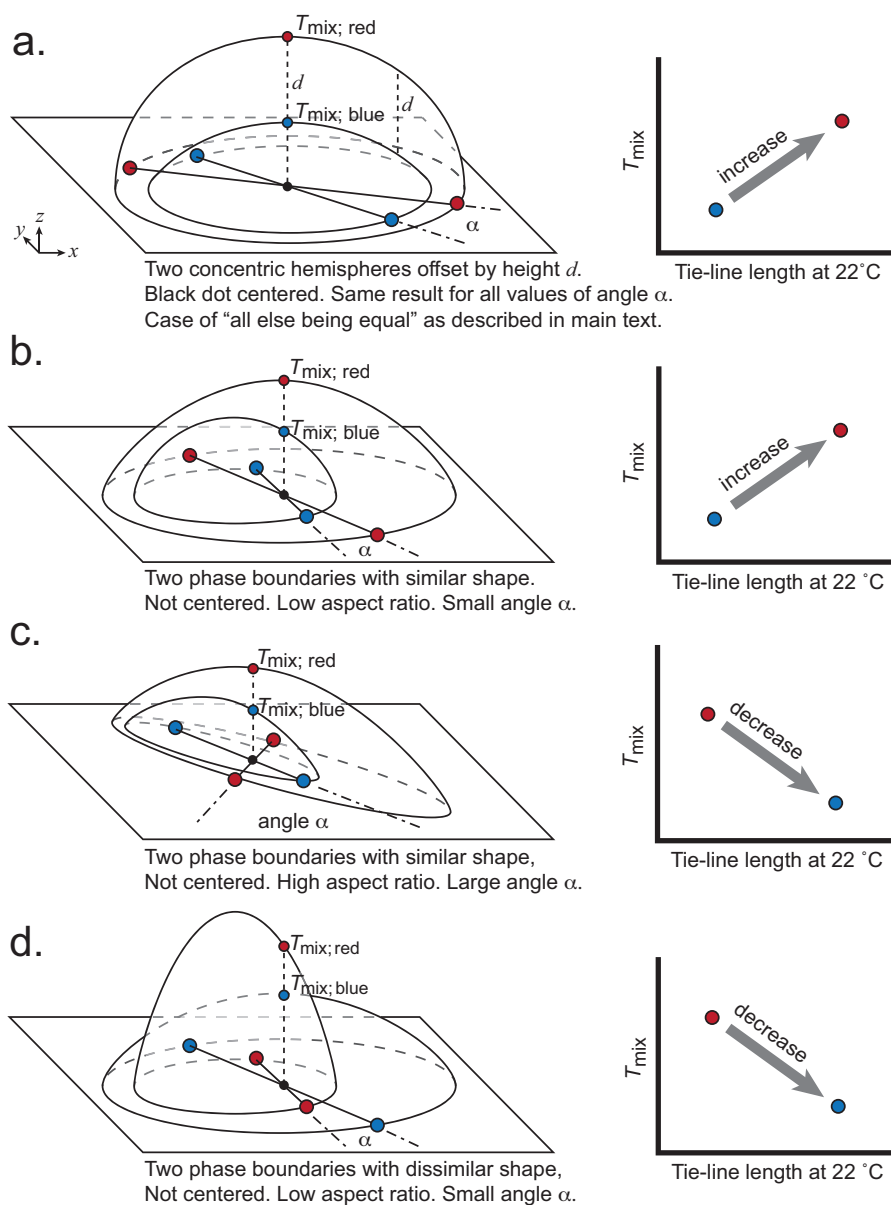
Figure S1

a.

Two concentric hemispheres offset by height d.
Black dot centered. Same result for all values of angle α.
Case of "all else being equal" as described in main text.

Tie-line length at 22˚C

b.

Two phase boundaries with similar shape.
Not centered. Low aspect ratio. Small angle α.

Tie-line length at 22 ˚C

c.

Two phase boundaries with similar shape,
Not centered. High aspect ratio. Large angle α.

Tie-line length at 22 ˚C

d.

Two phase boundaries with dissimilar shape,
Not centered. Low aspect ratio. Small angle α.

Tie-line length at 22 ˚C

Figure S1 Caption: Panels a – d show two curved surfaces, which represent miscibility phase boundaries of two different membranes, named "red" and "blue". The ratio of lipids within each membrane varies within the x-y plane. The experiment is conducted at a common, fixed ratio of the three lipid species in each membrane, at the black dot. The z-axis is temperature, where $z = 0$ is the experimental temperature, T_{mix}. Lipids within the red (blue) membrane demix into L_o and L_d phases at temperatures below $T_{mix; red}$ ($T_{mix; blue}$). At the temperature of the black dot, the ratios of lipid species in the L_o and L_d phases of the red (blue) membrane fall at the locations of the large red (blue) dots. The line that joins these large dots is the tie-line. Graphs at the right show relationships between miscibility transition temperatures and tie-line lengths for each of the four panels.

Table S1: Experimentally determined T_{mix} of lipid ratios that fall along a single tie-line

Mole % DiPhyPC/DPPC/Chol	Tmix (°C)
63.7 / 18.8 / 17.5	32.2 ± 0.5
58 / 22 / 20	34.4 ± 0.6
52.2 / 25.3 / 22.5	38.0 ± 1.1
46.5 / 28.5 / 25	40.2 ± 0.5
40.7 / 31.8 / 27.5	42.3 ± 0.7
35 / 35 / 30	45.3 ± 0.5
23.5 / 41.5 / 35	47.6 ± 0.1
12 / 48 / 40	48.7 ± 0.3

Tie-line compositions are interpolated from (9). Values of T_{mix} are reported as the temperature at which 50% of all vesicles have phase separated into L_o and L_d phases. Specifically, a sigmoidal fit is made of a plot of percent of vesicles that are phase separated vs. temperature. Reported experimental uncertainties in T_{mix} represent 95% confidence intervals of that sigmoidal fit.
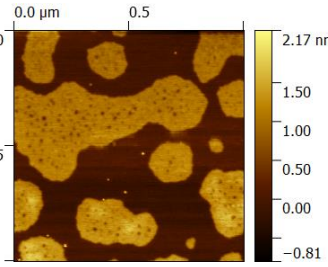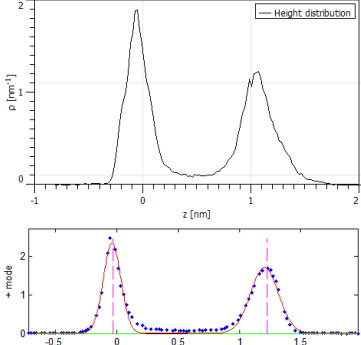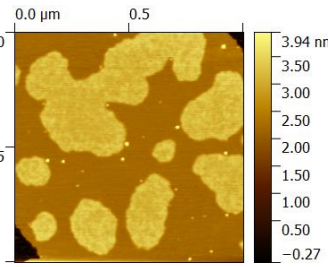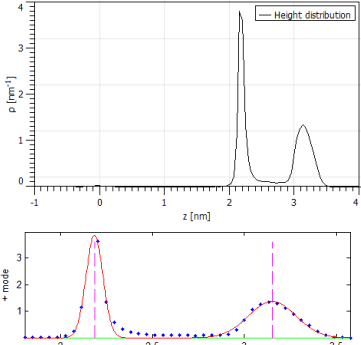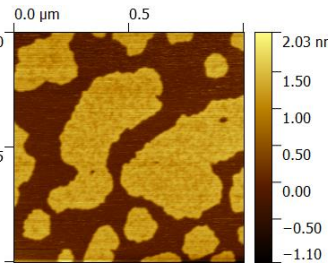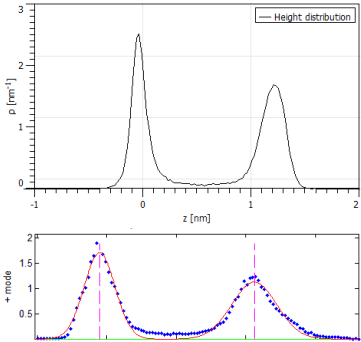
Table S2: Experimentally determined T_{mix} and Δh values

	Mole % DiPhyPC/DPPC/Chol	Tmix (°C)	Average Lo – Ld thickness (nm)
Tie-line Compositions			
a1	35 / 35 / 30	45.3 ± 0.5	0.94 ± 0.07
a2	46.5 / 28.5 / 25	40.2 ± 0.5	1.06 ± 0.05
a3	52.2 / 25.3 / 22.5	38.0 ± 1.1	1.03 ± 0.04
a4	63.7 / 18.8 / 17.5	32.2 ± 0.5	1.00 ± 0.03
Isothermal Compositions			
b1	27 / 23 / 50	41.0 ± 0.4	0.32 ± 0.002
b2	50 / 20 / 30	40.9 ± 1.2	1.03 ± 0.03
b3	46.5 / 28.5 / 25	40.2 ± 0.5	1.06 ± 0.05
b4	48 / 32 / 20	40.7 ± 0.3	1.43 ± 0.05

Values of T_{mix} are reported as the temperature at which 50% of all vesicles have phase separated into L_o and L_d phases. Specifically, a sigmoidal fit is made of a plot of percent of vesicles that are phase separated vs. temperature. Reported experimental uncertainties in T_{mix} represent 95% confidence intervals of that sigmoidal fit. Reported experimental uncertainties in average Lo-Ld thickness are the standard deviation of Lo-Ld thicknesses for at least three separate AFM scans.

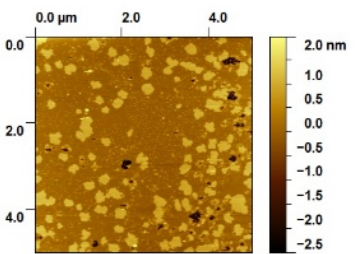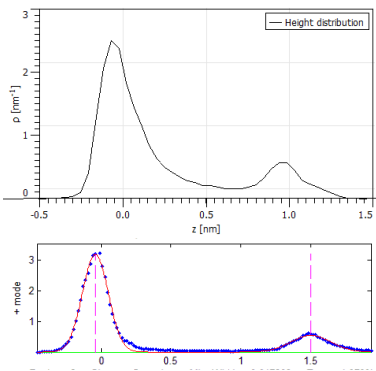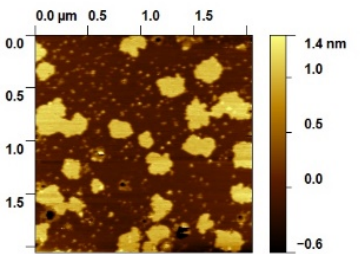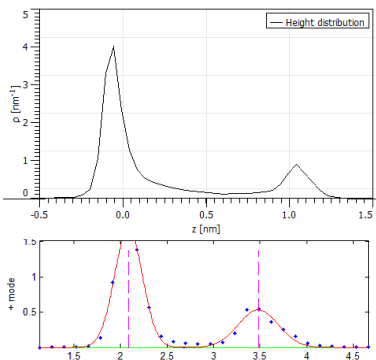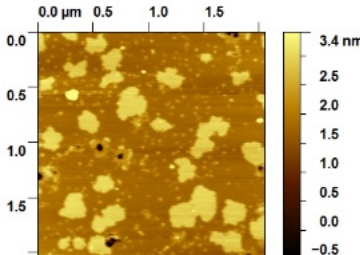**Table S3: AFM image, peak fits, and resulting data for 35/35/30 mole % DiPhyPC/DPPC/chol supported lipid bilayer**

#	AFM image[a]	(Top) height histogram[b] (Bottom) peak fit[c]	Difference in thickness between thin and thick membrane regions (nm)[d]	Ratio of areas of thick:thin regions[e]	Average thickness mismatch (nm)[f]; area ratio of thick:thin regions
1			0.757 ± 0.002	17:83	
2[g]			0.773 ± 0.002	20:80	
3			0.732 ± 0.006	45:55	0.94 ± 0.07 40:60 ± 15
4			1.018 ± 0.002	47:53	

5	0.0 µm 0.5 / 0.0 / 0.5 / 2.17 nm, 1.50, 1.00, 0.50, 0.00, −0.81	Height distribution	1.243 ± 0.001	53:47	
6	0.0 µm 0.5 / 0.0 / 0.5 / 3.94 nm, 3.50, 3.00, 2.50, 2.00, 1.50, 1.00, 0.50, −0.27	Height distribution	0.962 ± 0.008	50:50	
7	0.0 µm 0.5 / 0.0 / 0.5 / 2.03 nm, 1.50, 1.00, 0.50, 0.00, −0.50, −1.10	Height distribution	1.111 ± 0.002	49:51	

[a]Flattened AFM image with height scale bar in gold. [b]Height histogram in Gwyddion. [c]Typical peak fit trial of the height histogram in a 100-trial bootstrap fit. The dark red line shows the fit to the data marked by blue dots. Magenta dashed lines show the first guess at the peak position from the previous trial. [d]Difference between thickness of the thin and thick regions of the membrane reported as the mean difference in the location of the peaks determined by the bootstrap method. The reported uncertainty is the propagated standard deviation from the bootstrap fit of the two bilayer peaks. [e]Ratio of areas of thick and thin membrane regions from the bootstrap average areas of the two bilayer peaks. [f]Average thickness difference from column 4. The reported uncertainty is the standard error of the mean of the seven values. [g]Features far thicker than a lipid bilayer (the highest 12% of values) were excluded from the height histogram.
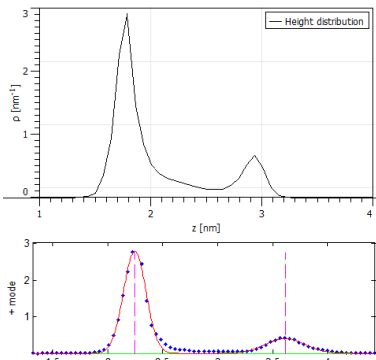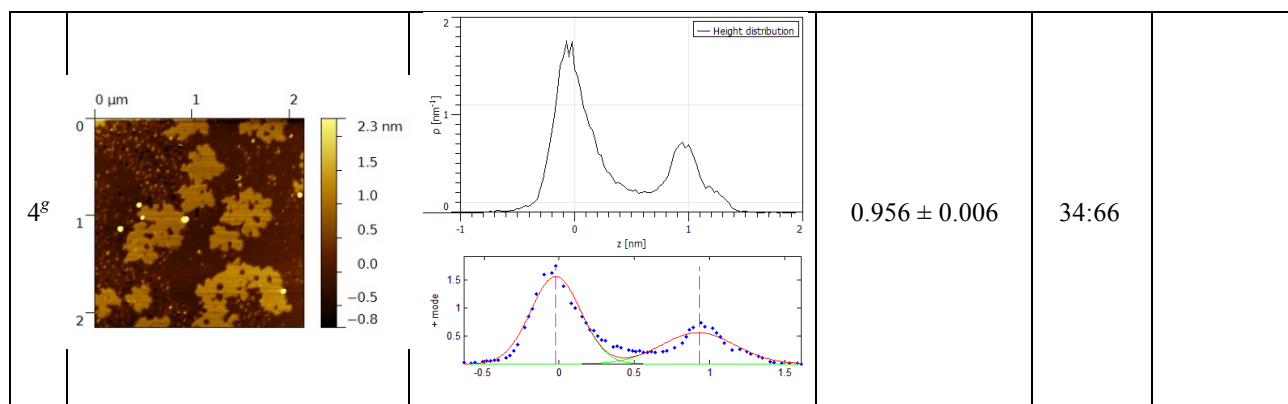
Table S4: AFM image, peak fits, and resulting data for 46.5/28.5/25 mole % DiPhyPC/DPPC/chol supported lipid bilayer

#	AFM image[a]	(Top) height histogram[b] (Bottom) peak fit[c]	Difference in thickness between thin and thick membrane regions (nm)[d]	Ratio of areas of thick:thin regions [e]	Avg. thickness mismatch (nm)[f]; area ratio of thick:thin regions
1[g]			0.952 ± 0.069	24:76	
2			1.093 ± 0.014	24:76	1.06 ± 0.05 24:76 ± 1
3[g]			1.129 ± 0.016	22:78	

[a]Flattened AFM image with height scale bar in gold. [b]Height histogram in Gwyddion. [c]Typical peak fit trial of the height histogram in a 100-trial bootstrap fit. The dark red line shows the fit to the data marked by blue dots. Magenta dashed lines show the first guess at the peak position from the previous trial. [d]Difference between thickness of the thin and thick regions of the membrane reported as the mean difference in the location of the peaks determined by the bootstrap method. The reported uncertainty is the propagated standard deviation from the bootstrap fit of the two bilayer peaks. [e]Ratio of areas of thick and thin membrane regions from the bootstrap average areas of the two bilayer peaks. [f]Average thickness difference from column 4. The reported uncertainty is the standard error of the three values. [g]Features far thicker than a lipid bilayer (the highest 12% of values) were excluded from the height histogram.

**Table S5: AFM image, peak fits, and resulting data for 52.2/25.3/22.5 mole %
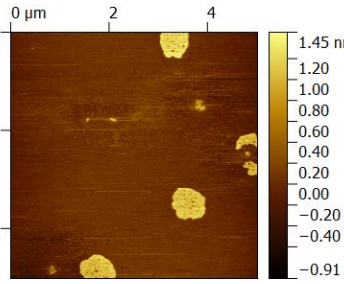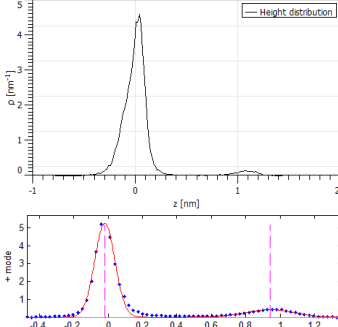DiPhyPC/DPPC/chol supported lipid bilayer**

#	AFM image[a]	(Top) height histogram[b] (Bottom) peak fit[c]	Difference in thickness between thin and thick membrane regions(nm)[d]	Ratio of areas of thick:thin regions[e]	Average thickness mismatch (nm)[f]; area ratio of thick:thin regions
1			0.952 ± 0.069	20:80	
2[g]			1.088 ± 0.003	21:79	1.03 ± 0.04 26:74 ± 4
3[h]			1.1067 ± 0.006	30:70	

				0.956 ± 0.006	34:66	
4[g]						

[a]Flattened AFM image with height scale bar in gold. [b]Height histogram in Gwyddion. [c]Typical peak fit trial of the height histogram in a 100-trial bootstrap fit. The dark red line shows the fit to the data marked by blue dots. Magenta dashed lines show the first guess at the peak position from the previous trial. [d]Difference between thickness of the thin and thick regions of the membrane reported as the mean difference in the location of the peaks determined by the bootstrap method. The reported uncertainty is the propagated standard deviation from the bootstrap fit of the two bilayer peaks. [e]Ratio of areas of thick and thin membrane regions from the bootstrap average areas of the two bilayer peaks. [f]Average thickness difference from column 4. The reported uncertainty is the standard error of the mean of the four values. [g]Features far thicker than a lipid bilayer (the highest 20% of values) were excluded from the height histogram. [h]Features far thicker than a lipid bilayer (the highest 12% of values) were excluded from the height histogram.

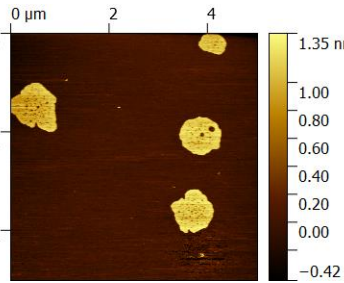**Table S6: AFM image, peak fits, and resulting data for 63.7/18.8/17.5 mole % DiPhyPC/DPPC/chol supported lipid bilayer**
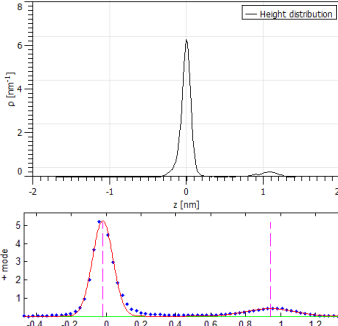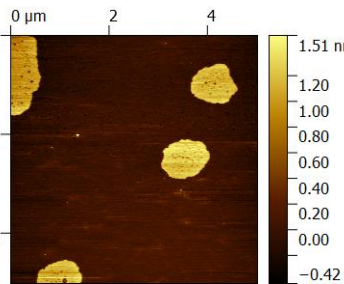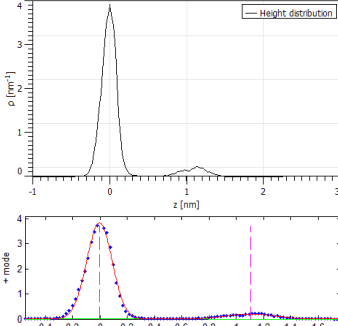
#	AFM image[a]	(Top) height histogram[b] (Bottom) peak fit[c]	Difference in thickness between thin and thick membrane regions (nm)[d]	Ratio of areas of thick:thin regions [e]	Average thickness mismatch (nm) [f] and area ratio of thick:thin regions
1			0.873 ± 0.002	13:87	
2			0.966 ± 0.001	18:82	1.00 ± 0.03 12:88 $\pm$ 5
3			0.959 ± 0.002	16:84	
4			0.979 ± 0.003	14:86	

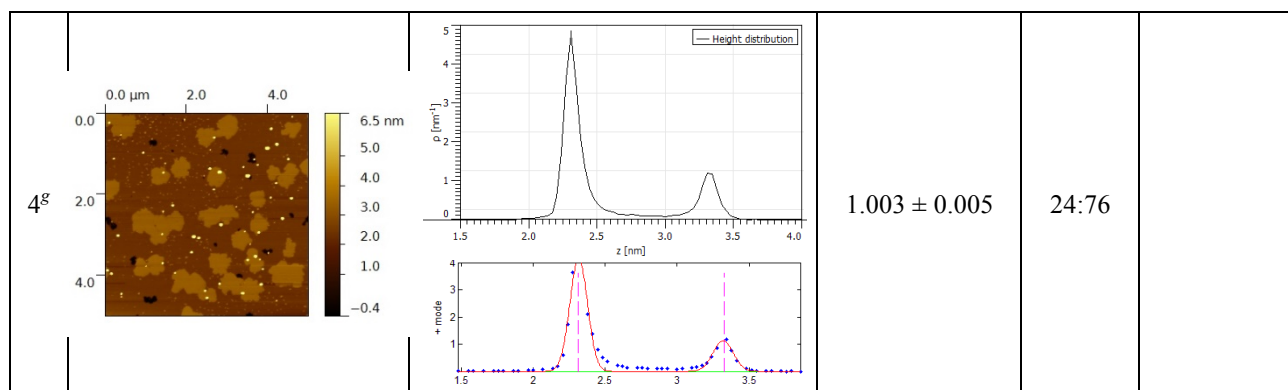|					
5			1.076 ± 0.003	4:96	
6			1.067 ± 0.003	8:92	
7			1.113 ± 0.003	9:91	

*a*Flattened AFM image with height scale bar in gold. *b*Height histogram in Gwyddion. *c*Typical peak fit trial of the height histogram in a 100-trial bootstrap fit. The dark red line shows the fit to the data marked by blue dots. Magenta dashed lines show the first guess at the peak position from the previous trial. *d*Difference between thickness of the thin and thick regions of the membrane reported as the mean difference in the location of the peaks determined by the bootstrap method. The reported uncertainty is the propagated standard deviation from the bootstrap fit of the two bilayer peaks. *e*Ratio of areas of thick and thin membrane regions from the bootstrap average areas of the two bilayer peaks. *f*Average thickness difference from column 4. The reported uncertainty is the standard error of the mean of the seven values.

Table S7: AFM image, peak fits, and resulting data for 27/23/50 mole % DiPhyPC/DPPC/chol supported lipid bilayer

#	AFM image[a]	(Top) height histogram[b] (Bottom) peak fit[c]	Difference in thickness between thin and thick membrane regions (nm)[d]	Ratio of areas of thick:thin regions[e]	Avg. thickness mismatch (nm)[f]; area ratio of thick:thin regions
1			0.322 ± 0.010	49:51	
2			0.316 ± 0.001	50:50	0.320 ± 0.002 $49:51 \pm 1$
3			0.321 ± 0.012	48:52	

[a]Flattened AFM image with height scale bar in gold. [b]Height histogram in Gwyddion. [c]Typical peak fit trial of the height histogram in a 100-trial bootstrap fit. The dark red line shows the fit to the data marked by blue dots. Magenta dashed lines show the first guess at the peak position from the previous trial. [d]Difference between thickness of the thin and thick regions of the membrane reported as the mean difference in the location of the peaks determined by the bootstrap method. The reported uncertainty is the propagated standard deviation from the bootstrap fit of the two bilayer peaks. [e]Ratio of areas of thick and thin membrane regions from the bootstrap average areas of the two bilayer peaks. [f]Average thickness difference from column 4. The reported uncertainty is the standard error of the mean of the three values. [g]Features far thicker than a lipid bilayer (the highest 20% of values) were excluded from the height histogram. [h]Features far thicker than a lipid bilayer (the highest 12% of values) were excluded from the height histogram.

Table S8: AFM image, peak fits, and resulting data for 50/30/20 mole % DiPhyPC/DPPC/chol supported lipid bilayer

#	AFM image[a]	(Top) height histogram[b] (Bottom) peak fit[c]	Difference in thickness between thin and thick membrane regions (nm)[d]	Ratio of areas of thick:thin regions[e]	Avg. thickness mismatch (nm)[f]; area ratio of thick:thin regions
1			1.002 ± 0.003	30:70	
2[g]			1.010 ± 0.004	29:71	1.003 ± 0.003 31:69 ± 7
3[g]			0.997 ± 0.003	41:59	

			1.003 ± 0.005	24:76	
4^g					

*Flattened AFM image with height scale bar in gold. *Height histogram in Gwyddion. *Typical peak fit trial of the height histogram in a 100-trial bootstrap fit. The dark red line shows the fit to the data marked by blue dots. Magenta dashed lines show the first guess at the peak position from the previous trial. *Difference between thickness of the thin and thick regions of the membrane reported as the mean difference in the location of the peaks determined by the bootstrap method. The reported uncertainty is the propagated standard deviation from the bootstrap fit of the two bilayer peaks. *Ratio of areas of thick and thin membrane regions from the bootstrap average areas of the two bilayer peaks. *Average thickness difference from column 4. The reported uncertainty is the standard error of the mean of the four values. *Features far thicker than a lipid bilayer (the highest 12% of values) were excluded from the height histogram.

Table S9: AFM image, peak fits, and resulting data for 48/32/20 mol %
DiPhyPC/DPPC/chol supported lipid bilayer

#	AFM image[a]	(Top) height histogram[b] (Bottom) peak fit[c]	Difference in thickness between thin and thick membrane regions (nm) [d]	Ratio of areas of thick:thin regions [e]	Avg. thickness mismatch (nm) [f]; area ratio of thick:thin regions
1			1.542 ± 0.001	21:79	
2			1.391 ± 0.022	31:69	1.43 ± 0.05 24:76 ± 6
3			1.370 ± 0.004	20:80	

[a]Flattened AFM image with height scale bar in gold. [b]Height histogram in Gwyddion. [c]Typical peak fit trial of the height histogram in a 100-trial bootstrap fit. The dark red line shows the fit to the data marked by blue dots. Magenta dashed lines show the first guess at the peak position from the previous trial. [d]Difference between thickness of the thin and thick regions of the membrane reported as the mean difference in the location of the peaks determined by the bootstrap method. The reported uncertainty is the propagated standard deviation from the bootstrap fit of the two bilayer peaks. [e]Ratio of areas of thick and thin membrane regions from the bootstrap average areas of the two bilayer peaks. [f]Average thickness difference from column 4. The reported uncertainty is the standard error of the mean of the three values.

Details of AFM image analysis

AFM image flattening using Gwyddion software

AFM images produce a false color topographic map, which are flattened in Gwyddion (12). The color is set to gold. Mean plane subtraction is used to eliminate background tilt that obscures bilayer thicknesses. Next, scan lines are corrected by matching height medians, and the image is corrected for horizontal scars. The mica and the lipid membrane, which may contain both thick and thin regions, produce at least two distinct height populations. To avoid non-physical flattening results due to these populations, we mask out each layer individually using the marks grains tool and perform a median line scan correction on each layer separately. Last, we mask out of the lowest feature, which is either the mica or thin membrane, and perform a background subtraction to set this feature to ~0 nm. We then use Gywddion's 1D statistical function to obtain the height histogram. We export height histogram values to excel, read the excel file into Matlab, and fit the data with peaks using a 100 bootstrap trial method as part of a Matlab peak fitting program named ifp.m (13).

Fitting AFM height histogram peaks to determine thickness mismatch

The interactive Matlab peak-fitting program ipf.m uses an unconstrained non-linear optimization algorithm to decompose separate and/or overlapping-peaks into component peaks (13). This process gives us differences in thickness between membrane regions, standard deviations in thickness, and areas of the peaks, which allows us to calculate the percent of the membrane area covered by thin and thick phases.

The default peak shape is a Gaussian. We find that changing peak type from Gaussian to other peak types, such as Lorentzian, results in larger fit errors and larger standard deviations from bootstrap methods. Running ipf.m produces a scatter plot of the height histogram data within an interactive graph. The user then selects the range of x-values (heights in nm) that encompasses all peaks of interest. The program requires first guesses for the peak positions, which is done automatically or by clicking on peaks. We used the clicking functionality because it is recommended for data like ours for which peaks are not evenly spaced. We next performed a 100 trial bootstrap fit. In each trial, the data set is divided into two sub-sets, each of which is fit, and then the process is repeated. The resulting standard deviation reflects the stability of the peak fit with respect to random noise in the data. Our reported values for thickness differences between thick and thin regions of membranes (Tables S3-S9) are the differences in the bootstrap mean value of the fitted peaks from the bootstrap fit. The reported uncertainties in the values for each image are the propagated errors from standard deviations produced by the bootstrap method. These values are averaged to give the average thickness mismatch (final column).

References for Supporting Information:

1.	Blosser, M. C.; Cornell, C.; Rayermann, S. P.; Keller, S. L., Phase Diagrams and Tie Lines in GUVs. In *The Giant Vesicle Book*, Dimova, R.; Marques, C., Eds. in press.
2.	Blosser, M. C.; Honerkamp-Smith, A. R.; Han, T.; Haataja, M.; Keller, S. L., Transbilayer Colocalization of Lipid Domains Explained Via Measurement of Strong Coupling Parameters. *Biophys. J.* **2015,** *109*, 2317-2327.
3.	Bleecker, J.V., Cox, P.A., Foster, R.N., Litz, J.P., Blosser, M.C., Castner, D.G., and Keller, S.L. **2015**. Thickness mismatch of non-canonical Lo-Ld lipid membranes. *J. Phys. Chem. B.* 120:2761-2770.
4.	Bhatia, T.; Husen, P.; Ipsen, J. H.; Bagatolli, L. A.; Simonsen, A. C., Fluid Domain Patterns in Free-Standing Membranes Captured on a Solid Support. *Biochim. Biophys. Acta* **2014,** *1838*, 2503-2510.
5.	Veatch, S. L.; Keller, S. L., Seeing Spots: Complex Phase Behavior in Simple Membranes. *Biochim. Biophys. Acta* **2005,** *1746*, 172-185.
6.	Hillert, M. *Phase equilibria, phase diagrams and phase transformations: their thermodynamic basis.* Cambridge University Press: Cambridge, 2007.
7.	Chaikin, P.M. and Lubensky, T.C. *Principles of condensed matter physics.* Cambridge University Press: Cambridge, 2000.
8.	Ferguson, F. D. and Jones, T. K. *The phase rule .* Butterworths: London, 1966.
9.	Veatch, S. L.; Gawrisch, K.; Keller, S. L., Closed-Loop Miscibility Gap and Quantitative Tie-Lines in Ternary Membranes Containing Diphytanoyl PC. *Biophys. J.* **2006,** *90*, 4428-4436.
10.	García-Sáez, A. J.; Chiantia, S.; Schwille, P., Effect of Line Tension on the Lateral Organization of Lipid Membranes. *J. Biol. Chem.* **2007,** *282*, 33537-33544.
11.	Connell, S. D.; Heath, G.; Olmsted, P. D.; Kisil, A., Critical Point Fluctuations in Supported Lipid Membranes. *Faraday Discuss.* **2013,** *161*, 91-111.
12.	Nečas, D.; Klapetek, P., Gwyddion: An Open-Source Software for SPM Data Analysis. *Cent. Eur. J. Phys.* **2012,** *10*, 181-188.
13.	O'Haver, T. ipf.m Peak Fitter: http://terpconnect.umd.edu/~toh/spectrum/ InteractivePeakFitter.htm.